European Organisation for Astronomical Research in the Southern Hemisphere
Observing Programmes Office • Karl-Schwarzschild-Strasse 2 • D-85748 Garching bei München • email: opo@eso.org • Tel: +49 89 3200 6473

DRAFT

Cycle: P106
Type: Normal
Status: Draft
Printed: 17 Apr 2020

APPLICATION FOR OBSERVING TIME

to be assigned

IMPORTANT NOTICE

Type Ia supernovae in low-luminosity host environments

ABSTRACT

Type Ia supernovae (SNIa) are the most accurate extragalactic distance indicators to date, thanks to empirical correlations between light-curve shape/B-V color and peak brightness that homogenize SNIa light-curves down to 7% scatter. However, it is now established that SNIa Hubble residuals correlate with global host galaxy parameters, such as total mass, and the addition of a term in the SNIa standardization accounting for these environmental parameters has reduced the scatter in the SNIa peak brightness. We aim to further study these correlations by using MUSE observations of host galaxies of well-studied SNe Ia selected from the Carnegie Supernova Project (CSP), to reduce further the scatter in the SNIa Hubble diagram by looking for correlations between Hubble residuals and both global and local galactic spectroscopic properties. With this proposal we plan to complete observations of the full CSP (I-II) sample by observing the remaining faint, low-mass host galaxies.

SCIENTIFIC CATEGORY

D5 Supernovae, pulsars

RUNS

Run	Period	Instrument	Tel. Setup	Constraints	Mode	Type	Propr. Time	Time Constr.	Req. Time
1. Run 1	106	MUSE	UT4	FLI: 100% • Turb.: 50% • pwv: 30.0mm • Sky: Variable, thin cirrus	SM	Normal	12m	×	53h00m

AWARDED AND FUTURE TIME REQUESTS

Time already awarded to this project

Instrument	Time	Comment
MUSE	34h	095.D-0091(A). SM. Only 23h executed. Data reduced and analysed.
MUSE	65h	095.D-0091(B). SM. All 65h executed. Data reduced and analysed.
MUSE	45h	098.D-0115(A). SM. Only 27h executed. Data reduced and analysed.
MUSE	99h	099.D-0022(A). SM. Only 35h executed. Data reduced and analysed.
MUSE	20h	101.D-0748(B). SM. Only 17h executed. Data reduced and analysed.
MUSE	99h	102.D-0095(A). SM. Only 44h executed. Data reduced and analysed.

Future time requests to complete this project

- none -

Special Remarks

This is a continuation project that aims to complete observations of SN Ia host galaxies from the Carnegie Supernova Project campaigns I and II taken in semesters P95, P98, P99, and P101 , and P102. Observations of this low-luminosity end galaxies are essential to the completion of the project, therefore we would also accept to perform the observations in filler mode, when the weather conditions are not optimal, and even spread over the P106 and P107 (we would send another proposal for this) periods.

DESCRIPTION OF THE PROPOSED PROGRAMME

A- Scientific Rationale

Optical observations of type Ia supernovae (SN Ia) have been widely used in the past decades to measure cosmological distances, and have been key in measuring the Hubble constant (Burns et al. 2018) and demonstrating cosmic acceleration (Riess et al. 1998; Perlmutter et al. 1999). Although SNe Ia show significant dispersion ($\sim$2.5 mag) in their absolute peak magnitudes in the optical, correlations among peak brightness, light curve (LC) shape, and observed color, enabled their standardization into the most precise (7%) extragalactic distance indicators.

The literature sample of optical SNe Ia at cosmological distances has grown substantially, and at this point statistical errors are comparable to systematic uncertainties (Brout et al. 2019). Further improvement in reducing these systematic errors require a much better understanding of the physical model of the explosion, which is still incomplete, a direct observational constraint on which kind of progenitors can produce SNe Ia, which is still lacking, as well as better control of reddening effects due to interstellar and/or circumstellar dust.

Optical studies of SNe Ia have now firmly established a dependence of Hubble diagram *residuals* ($\approx$ differences between distances estimated from SNe Ia peak brightness after correction for the luminosity-decline rate relation and those calculated assuming a fiducial cosmological model) on global *environmental* host galaxy parameters, such as mass, age, and metallicity (e.g. Sullivan et al. 2010, Rose et al. 2020). Moreover, these galaxy parameters might in principle correlate with the properties of the progenitor star, which might in turn influence the observational photometric and spectroscopic SN Ia properties. The addition of a term in the standardization of SNe Ia absolute magnitudes in the optical that accounts for these environmental properties (e.g. the 'mass step' or the γ-metallicity term; Moreno-Raya et al. 2016; Brout et al. 2019) has proved to further reduce the scatter of the Hubble residuals.

Most of these studies are based on analyses of the integrated or central host galaxy spectra or broad-band imaging. The effect of the *local environment* of SNe Ia within galaxies in cosmological studies remains largely unexplored. As an exception, Rigault et al. (2013, 2018) showed that SNe Ia exploding at locations with higher star-formation rate (SFR) intensity could be more standardizable than those in passive local environments. More recently, Roman et al. (2018) presented an analysis of the dependences of SN Ia LC parameters and Hubble residuals on their local environment using broad-band photometry. They show a significant dependence on the U-V color, which is treated as a proxy for the stellar age of the underlying populations (bluer being younger). However, age derived from photometry (color) has several uncertainties, and degeneracies (with extinction and stellar metallicity), and it is not enough to determine precisely the cut-out in stellar ages of such dependence.

A few semesters ago (P95), we started a program to go one step further by making use of the capabilities of Integral Field Spectroscopy (IFS) to search for correlations between SN Ia Hubble residuals and the properties of both their global and local environments (e.g., metallicity, age, SFR), through observing SN Ia host galaxies with MUSE. Our SN Ia sample was compiled from the Carnegie Supernova Project (CSP) campaigns I and II, that observed around 260 objects with the du Pont and Swope telescopes at Las Campanas Observatory (LCO) in Chile. These are unprecedented well-sampled light-curves in 6 optical and 3 near-infrared bands, in addition to optical and near-infrared spectra, which enables detailed photometric and spectroscopic analyses. MUSE observations allows a detailed characterization of both the global and the local environment of these SNe Ia, as well as the ability to then map galaxy-wide SN Ia host properties, and analyze where within the overall distribution of, e.g., host metallicity the SN Ia environment falls (see Galbany et al. 2018).

B- Immediate Objective

After five semesters collecting data with MUSE in filler mode, where observed targets are randomly selected, we aim here to complete and finalize the sample of CSP supernova hosts by obtaining data of the remaining galaxies that are located in the fainter end of the luminosity distribution, which in turn populate the low-mass and high-SFR region, making them essential to build a representative sample (see Figure 1, top-left panels).

We propose to obtain MUSE observations of the last 53 nearby ($z<0.1$) and low-luminosity SN Ia host galaxies, with high-quality optical and NIR SN observations from the CSP-I and -II, that are observable during P106. As shown in Figure 1 (right panels), a large aperture telescope and high throughput IFS is needed to obtain both gas-phase emission and underlying stellar continuum signal of these faint galaxies. This perfect combination provides both global host properties in addition to spectral information on the immediate environments of SNe Ia (and every single environment within the host). Using these observations, we will perform single stellar population (SSP) synthesis, and maps will be made of line-of sight ISM and stellar features, such as that of gas-phase and stellar metallicity, stellar age, and star-formation rate density (see details of the data analysis in Galbany et al. 2016). Together with the current sample of CSP hosts, this will allow a detailed and unprecedented study of the correlations between the SN Ia residuals to the ΛCDM cosmology in the Hubble diagram and both the global but especially the local environmental properties (See Figure 1, bottom-left panels).

The immediate goals of this proposal are: (i) Produce host-galaxy 2 dimensional maps of: light- and mass-weighted age (through both SSP modeling and Hα equivalent width measurements) and metallicity (through emission line ratios i.e. O3N2- and N2- calibrators, population modeling, and absorption lines when the S/N allows). SN Ia environments will then be placed within these distributions providing further progenitor constraints; and (ii) Look for correlations between the SN Ia residuals in the Hubble digram (assuming ΛCDM) and those local/global environmental properties, and use them to further refine the use of SNe Ia as precise distance indicators (Data from this proposal is essential to give significance to the correlations).

These remaining 53 galaxies are the faintest and with lowest-mass of the CSP-I -II sample, being essential to achieve our goals. Including low-luminosity galaxies will allow us to remove the bias in stellar mass of our current sample, recovering known trends in global properties such as the mass-step (SN Ia in high-mass galaxies have more negative Hubble residuals compared to SN Ia in low-mass galaxies; See top central panel in Figure 1), and enabling the exploration of their local environment. We also expect these observations to increase SNe Ia in low-metallicity environments, populating the low-metalliciy, young-age, high-SFR and high Hα EW correlations with SN Ia properties, and improving their significance by extending the current parameter range, (See lower panels in Figure 1). **Without these objects, the project cannot be completed.** This dataset will also have a legacy value for further study; it will be extremely useful for studies of galaxy dynamics, stellar populations and chemical evolution, and hence we expect many other projects to spawn from the dataset. In particular, and similarly to our project, these data will be of interest for other researchers aiming to include dwarf and low-mass, low-metallicity galaxies in their statistcal samples. Note that our group has already published 18 papers using data obtained in previous semesters, either directly related to SN environments or about galaxy enrichment and evolution.

Figures

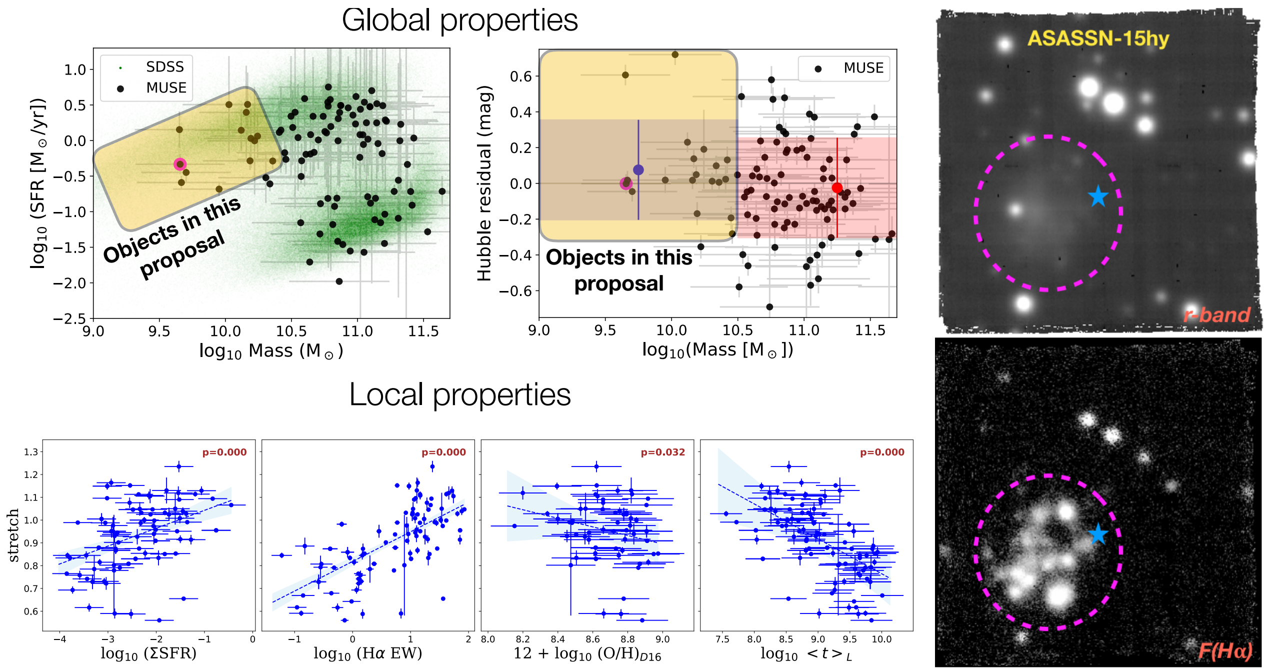

Fig. 1: *Left Upper panels.* **GLOBAL** SFR vs stellar mass, and SN Ia Hubble residual vs stellar mass diagrams from MUSE data obtained in semesters P95 to P102, on top of the SDSS galaxy distribution (Galbany et al. in prep.). The yellow area in both panels represent the region the observations requested in this proposal will cover. It can clearly be seen that currently we are lacking of galaxies in the lower mass end, which are needed to recover the correlations seen in the literature in the **GLOBAL** SFR-mass relation, and the SN Ia 'mass step'. *Bottom left panels.* Current correlations between the SN Ia stretch and a number of galactic properties measured at the SN 1kpc^2 **LOCAL** environment. We currently find significant relations, but find insignificant correlations between the same galactic parameters and either SN color or SN Ia Hubble residuals. We expect those correlations to appear when adding SNe in very low-luminosity low-metallicity galaxies. *Right panels.* Example of a faint low-mass galaxy (marked in purple in the upper left panels), that is not clearly seen in the MUSE synthetic r-band image but that pops-up in the pure Hα emission line map produced by our pipeline. It is crucial to include these kind of object in our analysis, otherwise our results would be biased towards bright high-mass galaxies.

References

Brout et al. 2019, ApJ, 874, 150; Burns et al. 2018, ApJ, 869, 56; Galbany et al., 2016, A&A, 591, 48; Galbany et al., 2018, ApJ, 855, 107; Moreno-Raya et al. 2016, 2016, ApJ, 818, 19; Perlmutter et al. 1999, ApJ, 517, 565; Riess et al 1996, 473, 88; Rigault et al. 2013, A&A, 560, 66; Rigault et al. 2018, astro-ph:1806.03849; Roman et al. 2018, A&A, 615, 68; Rose et al. 2020, ApJ. 890, 60; Sullivan et al 2010, MNRAS, 406, 782;

TARGETS

Name	RA	Dec	Coord	Runs	Comment
SN2008bf	12:04:02.90	+20:14:42.6	J2000	1	
SN2007if	01:10:51.37	+15:27:39.9	J2000	1	
SN2008fr	01:11:49.14	+14:38:27.0	J2000	1	
SN2009al	10:51:22.07	+08:34:42.7	J2000	1	
SN2009ab	04:16:36.39	+02:45:51.0	J2000	1	
SN2007jh	03:36:01.54	+01:06:12.2	J2000	1	
SN2007jg	03:29:50.82	+00:03:24.6	J2000	1	
SN2005cf	15:21:33.12	-07:26:57.1	J2000	1	
SN2009F	04:59:23.56	-11:07:50.1	J2000	1	
SN2008R	03:03:53.70	-11:59:39.4	J2000	1	
SN2008bt	10:50:16.88	-12:06:32.0	J2000	1	
SN2005el	05:11:48.72	+05:11:39.4	J2000	1	
KISS13l	11:14:54.07	+29:35:06.00	J2000	1	
KISS15n	13:00:32.33	+27:58:41.00	J2000	1	
CSP14adc	02:26:23.31	+27:39:34.80	J2000	1	
SN2012aq	14:54:05.13	+22:05:40.60	J2000	1	
KISS13v	13:52:56.63	+21:56:21.70	J2000	1	
KISS15m	12:06:00.83	+20:36:18.40	J2000	1	
LSQ14mc	09:02:13.45	+17:03:37.01	J2000	1	
KISS13j	12:09:39.70	+16:12:14.30	J2000	1	
PTF13efe	08:43:39.30	+16:10:37.30	J2000	1	
PTF13anh	13:06:50.45	+15:34:32.36	J2000	1	
CSP14aal	09:57:39.11	+12:33:17.70	J2000	1	
PTF13dwl	21:16:49.05	+12:00:50.80	J2000	1	
SN2013ad	03:38:41.04	+10:18:27.22	J2000	1	
CSP13aaf	09:55:08.22	+06:48:31.40	J2000	1	
CSP13abm	03:05:59.89	+04:32:38.20	J2000	1	
SN2013ct	01:12:54.92	+00:58:45.70	J2000	1	
CSP13abs	12:03:06.88	-01:01:31.70	J2000	1	
LSQ14gfn	03:28:32.16	-04:12:14.22	J2000	1	
SN2013gy	03:42:16.88	-04:43:18.48	J2000	1	
LSQ11bk	04:20:44.25	-08:35:55.75	J2000	1	
LSQ12btn	09:21:30.47	-09:41:29.86	J2000	1	
CSP14acl	01:01:07.04	-10:18:39.90	J2000	1	
CSP13Z	10:52:06.06	-13:34:24.70	J2000	1	
ASASSN-15go	06:11:30.50	-16:29:03.52	J2000	1	
LSQ12hjm	03:10:28.72	-16:29:37.08	J2000	1	
CSP13V	10:13:10.00	-16:31:54.00	J2000	1	
LSQ12gyc	02:45:50.07	-17:55:45.74	J2000	1	
ASASSN-14lq	22:57:19.41	-20:58:00.8	J2000	1	
ASASSN-15da	05:23:51.880	-24:42:08.38	J2000	1	
SN2014I	05:42:19.80	-25:32:39.90	J2000	1	
LSQ14ghv	03:23:44.15	-31:35:03.17	J2000	1	
LSQ14fms	00:14:59.82	-51:12:39.54	J2000	1	
CSP13aay	03:25:33.51	-53:44:19.00	J2000	1	

Name	RA	Dec	Coord	Runs	Comment
SN2012U	02:06:04.33	-55:11:37.50	J2000	1	
SN2014eg	02:45:09.27	-55:44:16.90	J2000	1	
SN2014Z	01:44:07.99	-61:07:07.40	J2000	1	
CSP14acy	00:42:28.75	-64:45:51.00	J2000	1	
ASASN-14mw	01:41:25.16	-65:37:01.26	J2000	1	
CSP13aam	05:14:47.50	-66:50:29.10	J2000	1	
SN2015F	07:36:15.76	-69:30:23.00	J2000	1	
CSP15aae	14:09:55.13	+17:31:55.60	J2000	1	

Target Notes

These 53 targets (12 from the CSP-I and 41 from the CSP-II) are the remaining objects from the 264 of the total sample. The particularity of these SNe is that they occurred in a very low-luminosity galaxy or are hostless (= galaxy undetected in DSS archival images). For the former, a 8m telescope and a high-throughput instrument are needed to get sufficient S/N spectroscopic data of the hosts, while for the latter we expect to find/discover the SN host galaxy from their brighter gas-emission lines, as we have already show in Galbany et al. (2018; MNRAS, 479, 262-274) and Anderson et al. (2018; NatAs, 2, 574-579).

REMARKS & JUSTIFICATIONS

Lunar Phase and Constraints Justification

Please justify here the requested lunar phase and other observing constraints.

Although we prefer dark/grey time to enhance the S/N, our targets can be observed in any lunar phase. In the worst case we will spatially bin the datacube.

Time Justification

Please describe here a detailed computation of the necessary time to execute the observations, including time-critical aspects if any. Parameters used in the ETC should be mentioned so the computation can be reproduced.

Our proposed MUSE observations aim to detect and measure the strength of H II region emission lines throughout target galaxies, together with narrow absorption features seen on top of the galaxy continuum. To estimate exposure times, we assume a typical r-band surface brightness of 21 mag per arcsec^2 for faint HII regions (James et al. 2004). We then use the MUSE ETC to estimate our required exposure times. We assume an 'Infinitely extended source' and the HII region template (at a redshift of 0.05) together with an r-band surface brightness of 21 mag per arcsec^2. As a 'filler' proposal we set conditions to 7 days from new moon with an airmass of 1.4 and seeing 1.5″.

In order to remove the edges of each IFU on the detector (artifacts of the image slicer) it is best to combine observations with all four 90 degree angles. With 4×700 second exposures the ETC gives a S/N of ~5 in the continuum, which translates to a S/N of more than 100 for all the emission lines we wish to detect (e.g., Hα, [Nii], [O iii], Hβ). In many galaxy regions we will obtain much higher S/N in the continuum, and this will allow more detailed analysis of stellar populations, using absorption line indices as an indicator of stellar metallicities in place of the gas phase values, for the small number of elliptical galaxies expected in our sample. This totals roughly 1 hr per galaxy.

Most galaxies in our sample are covered by one MUSE pointing, so we require 53 hrs to observe our sample of 53 host galaxies. We have previously obtained MUSE data with very similar conditions/observing strategy to that outlined above, and with the above exposure times we are able to make the necessary measurements. We have already published several (18) papers based on these data (see publications section). Our team has experts on the reduction, analysis and interpretation of IFS galaxy observations, hence, while IFS data and their analysis can sometimes prove somewhat daunting, our team provides all the required knowledge to fully exploit this rich data set. These data will remain in the archive as a legacy for future extragalactic studies.

Telescope Justification

Please justify why the telescope requested is the best choice for this programme.

MUSE at the VLT is the only currently available IFU instrument that has a FoV of sufficient size to cover the majority of our targets, while at the same time having high spatial resolution, high sensitivity, and being extremely efficient, hence enabling targets to be observed in a relatively small amount of time.

We stress here that even in relatively bad seeing conditions we will still have the potential to unravel kinematic and population substructure in these galaxies over a large FoV. Indeed, even in bad seeing conditions these data will still be better-positioned to probe SN environments and galaxy characteristics than any current or past IFU survey (SAURON, ATLAS3D, CALIFA, SAMI, MaNGA).

Observing Mode Justification

Please justify the choice of SM, VM or dVM.

Targets are observable throughout the semester, so service mode is required.

Calibration Request

If you need any special calibration not included in the instrument calibration plan, please specify it here.

Standard Calibration

Duplication with ESO Science Archive

If observations of the same target(s) using the same instrument(s) already exist in the ESO archive, please justify why this programme requests further observations.

We searched for duplications, and there are no IFU observations of these galaxies in the ESO or any other public archive.

GTO & Survey Target Duplication Justification

If an instrument GTO or Public Survey team aims at the same target(s), please justify why this programme requests further observations.

N/A

Background and Expertise

Short description of the background, expertise and roles of the various team members in the context of the science case discussed in the proposal. For small teams the applicants may wish to provide a sentence for the qualifications of each member, while for larger teams (e.g. in Large Programmes), only the leading roles need to be specified.

The team has acquired and analysed the vast majority of VLT/MUSE observations of supernova host galaxies. We have tools in place to rapidly leverage the scientific yield of this combined data set. The team is committed to public releases of the analysis, and it will form an integral part of the larger data release framework for our MUSE survey (AMUSING DR1 expected for July 2020 during EAS virtual 2020 meeting).

L. Galbany is an expert in studying various supernovae and their host galaxies with integral field spectrograph (IFS) data. He has led and published several works from different campaigns on SNe and their host galaxies, and has expertise in the scheduling, reduction and analysis of VLT data.
J. P. Anderson has previously led the AMUSING proposals, and thus has significant experience of data and project organisation. He has expertise in supernova environment studies and how those studies can constrain progenitor scenarios.
S. F. Sanchez is an expert in galaxy formation and evolution, particularly through the use of spectral synthesis with IFS data, and will lead galaxy work on the data.
M. M. Phillips and M. Stritzinger are founder members of the Carnegie Supernova Project and will provide expertise in SN Ia light curve fitting.
H. Kuncarayakti has led MUSE core-collpse SN host galaxies projects (AMUSING, FOSSIL), and is an expert on analysing IFU data.
M. Smith and S. González-Gaitán are SN Ia cosmology experts and led several analyses in large SN surveys (SDSS, SNLS, DES).
Collectively, the team has ~70 first author papers on topics related to the proposal in the last 5 years, gathering over 2000 citations.

REPORT ON PREVIOUS USAGE OF ESO FACILITIES

Run	PI	Instrument	Time	Mode	Comment
095.D-0091(A)	Joseph Anderson	MUSE	34.0h	Service	Data reduced. 18 publications. Data from the current proposal is needed to finalize the project.
MUSE observations of Type Ia supernova environments: constraining progenitor properties, and refining distance calibration techniques					
095.D-0091(B)	Joseph Anderson	MUSE	65.0h	Service	Data reduced. 18 publications. Data from the current proposal is needed to finalize the project.
MUSE observations of Type Ia supernova environments: constraining progenitor properties, and refining distance calibration techniques					
098.D-0115(A)	Lluis Galbany	MUSE	45.0h	Service	Data reduced. 18 publications. Data from the current proposal is needed to finalize the project.
The All-weather MUse Supernova Integral field Nearby Galaxies (AMUSING) survey IV: Reducing the scatter in the Near Infrared SN Ia Hubble diagram					
099.D-0022(A)	Lluis Galbany	MUSE	99.0h	Service	Data reduced. 18 publications. Data from the current proposal is needed to finalize the project.
The All-weather MUse Supernova Integral field Nearby Galaxies (AMUSING) survey V: Host galaxy dependences in the Near Infrared SN Ia Hubble diagram					
0101.D-0748(B)	Hanindyo Kuncarayakti	MUSE	20.0h	Service	Data reduced. 18 publications. Data from the current proposal is needed to finalize the project.
The All-weather MUse Supernova Integral field Nearby Galaxies (AMUSING) survey VII: Continuing the survey of nebular spectra and environments of core-collapse supernovae					
0102.D-0095(A)	Joseph Anderson	MUSE	99.0h	Service	Data reduced. 18 publications. Data from the current proposal is needed to finalize the project.
The All-weather MUse Supernova Integral field Nearby Galaxies (AMUSING) survey VIII: The local environments of type Ia supernovae					
0104.D-0498(A)	Lluis Galbany	KMOS	36.0h	Service	Data reduced. Analysis ongoing.
Studying the local environment of type Ia supernovae at low and high redshift with the Dark Energy Survey					

RECENT PI/CoIs PUBLICATIONS MOST RELEVANT TO THE SUBJECT OF THIS PROPOSAL

1. Sánchez-Menguiano, L., Sánchez, S. F., Pérez, I., et al. (2018) "The shape of oxygen abundance profiles explored with MUSE: evidence for widespread deviations from single gradients," A&A, 609, A119 - 2018A&A...609A.119S

2. Boselli, A., Fossati, M., Consolandi, G., et al. (2018) "A Virgo Environmental Survey Tracing Ionised Gas Emission (VESTIGE). IV. A tail of

ionised gas in the merger remnant NGC4424," A&A, 620, A164 - 2018A&A...620A.164B

3. Anderson, J. P., Dessart, L., Gutiérrez, C. P., et al. (2018) "The lowest-metallicity type II supernova from the highest-mass red supergiant progenitor," NatAs, 2, 574-579 - 2018NatAs...2..574A
4. Galbany, L., Collett, T. E., Méndez-Abreu, J., et al. (2018) "Serendipitous discovery of a strong-lensed galaxy in integral field spectroscopy from MUSE," MNRAS, 479, 262-274 - 2018MNRAS.479..262G
5. Kuncarayakti, H., Anderson, J. P., Galbany, L., et al. (2018) "Constraints on core-collapse supernova progenitors from explosion site integral field spectroscopy," A&A, 613, A35 - 2018A&A...613A..35K
6. Phillips, M. M., Contreras, C., Hsiao, E. Y., et al. (2019) "Carnegie Supernova Project-II: Extending the Near-infrared Hubble Diagram for Type Ia Supernovae to z ˜0.1," PASP, 131, 014001 - 2019PASP..131a4001P
7. Lyman, J. D., Taddia, F., Stritzinger, M. D., et al. (2018) "Investigating the diversity of supernovae type Iax: a MUSE and NOT spectroscopic study of their environments," MNRAS, 473, 1359-1387 - 2018MNRAS.473.1359L
8. Bellocchi, E., Ascasibar, Y., Galbany, L., et al. (2019) "Uncertainties in gas kinematics arising from stellar continuum modeling in integral field spectroscopy data: the case of NGC 2906 observed with VLT/MUSE," A&A, 625, A83 - 2019A&A...625A..83B
9. Sánchez-Menguiano, L., Sánchez, S. F., Pérez, I., et al. (2020) "Arm-interarm gas abundance variations explored with MUSE: the role of spiral structure in the chemical enrichment of galaxies," MNRAS, 492, 4149-4163 - 2020MNRAS.492.4149S
10. López-Cobá, C., Sánchez, S. F., Anderson, J. P., et al. (2020) "The AMUSING++ Nearby Galaxy Compilation: I. Full Sample Characterization and Galactic--Scale Outflows Selection," arXiv, arXiv:2002.09328 - 2020arXiv200209328L

INVESTIGATORS

Lluis Galbany, Universidad de Granada, Spain (PI)
Mark Phillips, Carnegie Observatories, United States
Joseph Anderson, ESO Chile, ESO
Mathew Smith, University of Southampton, United Kingdom
Hanindyo Kuncarayakti, Turun yliopisto, Finland
Santiago Gonzalez, Universidade de Lisboa, Portugal
Maximilian Stritzinger, University of Aarhus, Denmark
S. Sanchez, Universidad Nacional Autónoma de México, Mexico

OBSERVATIONS

In the table below, the repeat factor is applied to the complete observation on that target, including its overhead.

✔ The PI acknowledged that all the telescope times listed below include overheads.

1. Run 1 • P106 • MUSE • SM — Tel. Time: 53h00m

FLI: 100% • Turb.: 50% • pwv: 30.0mm • Sky: Variable, thin cirrus • Airmass: 2.0

Target • SN2008bf • 12:04:02.90 • +20:14:42.6 — Tel. Time: 01h00m

OS 1	WFM-NOAO	Observation
Tel. Time: 900 s	Instrument Mode: WFM-NOAO-E	Integration Time: 0 s
Repeat: 4 x	Telescope Overheads: 360 s	Instrument Overheads: 0 s
Total Tel. Time: 3600s		Signal/Noise: 0.0

Target • SN2007if • 01:10:51.37 • +15:27:39.9 — Tel. Time: 01h00m

OS 1	WFM-NOAO	Observation
Tel. Time: 900 s	Instrument Mode: WFM-NOAO-E	Integration Time: 0 s
Repeat: 4 x	Telescope Overheads: 360 s	Instrument Overheads: 0 s
Total Tel. Time: 3600s		Signal/Noise: 0.0

Target • SN2008fr • 01:11:49.14 • +14:38:27.0 — Tel. Time: 01h00m

OS 1	WFM-NOAO	Observation
Tel. Time: 900 s	Instrument Mode: WFM-NOAO-E	Integration Time: 0 s
Repeat: 4 x	Telescope Overheads: 360 s	Instrument Overheads: 0 s
Total Tel. Time: 3600s		Signal/Noise: 0.0

Target • SN2009al • 10:51:22.07 • +08:34:42.7 — Tel. Time: 01h00m

OS 1	WFM-NOAO	Observation
Tel. Time: 900 s	Instrument Mode: WFM-NOAO-E	Integration Time: 0 s
Repeat: 4 x	Telescope Overheads: 360 s	Instrument Overheads: 0 s

Total Tel. Time: 3600s		Signal/Noise: 0.0

Target • SN2009ab • 04:16:36.39 • +02:45:51.0 Tel. Time: 01h00m

OS 1	WFM-NOAO	Observation
Tel. Time: 900 s	Instrument Mode: WFM-NOAO-E	Integration Time: 0 s
Repeat: 4 x	Telescope Overheads: 360 s	Instrument Overheads: 0 s
Total Tel. Time: 3600s		Signal/Noise: 0.0

Target • SN2007jh • 03:36:01.54 • +01:06:12.2 Tel. Time: 01h00m

OS 1	WFM-NOAO	Observation
Tel. Time: 900 s	Instrument Mode: WFM-NOAO-E	Integration Time: 0 s
Repeat: 4 x	Telescope Overheads: 360 s	Instrument Overheads: 0 s
Total Tel. Time: 3600s		Signal/Noise: 0.0

Target • SN2007jg • 03:29:50.82 • +00:03:24.6 Tel. Time: 01h00m

OS 1	WFM-NOAO	Observation
Tel. Time: 900 s	Instrument Mode: WFM-NOAO-E	Integration Time: 0 s
Repeat: 4 x	Telescope Overheads: 360 s	Instrument Overheads: 0 s
Total Tel. Time: 3600s		Signal/Noise: 0.0

Target • SN2005cf • 15:21:33.12 • -07:26:57.1 Tel. Time: 01h00m

OS 1	WFM-NOAO	Observation
Tel. Time: 900 s	Instrument Mode: WFM-NOAO-E	Integration Time: 0 s
Repeat: 4 x	Telescope Overheads: 360 s	Instrument Overheads: 0 s
Total Tel. Time: 3600s		Signal/Noise: 0.0

Target • SN2009F • 04:59:23.56 • -11:07:50.1 Tel. Time: 01h00m

OS 1	WFM-NOAO	Observation
Tel. Time: 900 s	Instrument Mode: WFM-NOAO-E	Integration Time: 0 s
Repeat: 4 x	Telescope Overheads: 360 s	Instrument Overheads: 0 s
Total Tel. Time: 3600s		Signal/Noise: 0.0

Target • SN2008R • 03:03:53.70 • -11:59:39.4 Tel. Time: 01h00m

OS 1	WFM-NOAO	Observation
Tel. Time: 900 s	Instrument Mode: WFM-NOAO-E	Integration Time: 0 s
Repeat: 4 x	Telescope Overheads: 360 s	Instrument Overheads: 0 s
Total Tel. Time: 3600s		Signal/Noise: 0.0

Target • SN2008bt • 10:50:16.88 • -12:06:32.0 Tel. Time: 01h00m

OS 1	WFM-NOAO	Observation
Tel. Time: 900 s	Instrument Mode: WFM-NOAO-E	Integration Time: 0 s
Repeat: 4 x	Telescope Overheads: 360 s	Instrument Overheads: 0 s
Total Tel. Time: 3600s		Signal/Noise: 0.0

Target • SN2005el • 05:11:48.72 • +05:11:39.4 Tel. Time: 01h00m

OS 1	WFM-NOAO	Observation
Tel. Time: 900 s	Instrument Mode: WFM-NOAO-E	Integration Time: 0 s
Repeat: 4 x	Telescope Overheads: 360 s	Instrument Overheads: 0 s
Total Tel. Time: 3600s		Signal/Noise: 0.0

Target • KISS13l • 11:14:54.07 • +29:35:06.00 Tel. Time: 01h00m

OS 1	WFM-NOAO	Observation
Tel. Time: 900 s	Instrument Mode: WFM-NOAO-E	Integration Time: 0 s
Repeat: 4 x	Telescope Overheads: 360 s	Instrument Overheads: 0 s
Total Tel. Time: 3600s		Signal/Noise: 0.0

Target • KISS15n • 13:00:32.33 • +27:58:41.00 Tel. Time: 01h00m

OS 1	WFM-NOAO	Observation
Tel. Time: 900 s	Instrument Mode: WFM-NOAO-E	Integration Time: 0 s
Repeat: 4 x	Telescope Overheads: 360 s	Instrument Overheads: 0 s
Total Tel. Time: 3600s		Signal/Noise: 0.0

Target • CSP14adc • 02:26:23.31 • +27:39:34.80 Tel. Time: 01h00m

OS 1	WFM-NOAO	Observation
Tel. Time: 900 s	Instrument Mode: WFM-NOAO-E	Integration Time: 0 s

Repeat: 4 x Total Tel. Time: 3600s	Telescope Overheads: 360 s	Instrument Overheads: 0 s Signal/Noise: 0.0

Target • SN2012aq • 14:54:05.13 • +22:05:40.60 — Tel. Time: 01h00m

OS 1	WFM-NOAO	Observation
Tel. Time: 900 s Repeat: 4 x Total Tel. Time: 3600s	Instrument Mode: WFM-NOAO-E Telescope Overheads: 360 s	Integration Time: 0 s Instrument Overheads: 0 s Signal/Noise: 0.0

Target • KISS13v • 13:52:56.63 • +21:56:21.70 — Tel. Time: 01h00m

OS 1	WFM-NOAO	Observation
Tel. Time: 900 s Repeat: 4 x Total Tel. Time: 3600s	Instrument Mode: WFM-NOAO-E Telescope Overheads: 360 s	Integration Time: 0 s Instrument Overheads: 0 s Signal/Noise: 0.0

Target • KISS15m • 12:06:00.83 • +20:36:18.40 — Tel. Time: 01h00m

OS 1	WFM-NOAO	Observation
Tel. Time: 900 s Repeat: 4 x Total Tel. Time: 3600s	Instrument Mode: WFM-NOAO-E Telescope Overheads: 360 s	Integration Time: 0 s Instrument Overheads: 0 s Signal/Noise: 0.0

Target • LSQ14mc • 09:02:13.45 • +17:03:37.01 — Tel. Time: 01h00m

OS 1	WFM-NOAO	Observation
Tel. Time: 900 s Repeat: 4 x Total Tel. Time: 3600s	Instrument Mode: WFM-NOAO-E Telescope Overheads: 360 s	Integration Time: 0 s Instrument Overheads: 0 s Signal/Noise: 0.0

Target • KISS13j • 12:09:39.70 • +16:12:14.30 — Tel. Time: 01h00m

OS 1	WFM-NOAO	Observation
Tel. Time: 900 s Repeat: 4 x Total Tel. Time: 3600s	Instrument Mode: WFM-NOAO-E Telescope Overheads: 360 s	Integration Time: 0 s Instrument Overheads: 0 s Signal/Noise: 0.0

Target • PTF13efe • 08:43:39.30 • +16:10:37.30 — Tel. Time: 01h00m

OS 1	WFM-NOAO	Observation
Tel. Time: 900 s Repeat: 4 x Total Tel. Time: 3600s	Instrument Mode: WFM-NOAO-E Telescope Overheads: 360 s	Integration Time: 0 s Instrument Overheads: 0 s Signal/Noise: 0.0

Target • PTF13anh • 13:06:50.45 • +15:34:32.36 — Tel. Time: 01h00m

OS 1	WFM-NOAO	Observation
Tel. Time: 900 s Repeat: 4 x Total Tel. Time: 3600s	Instrument Mode: WFM-NOAO-E Telescope Overheads: 360 s	Integration Time: 0 s Instrument Overheads: 0 s Signal/Noise: 0.0

Target • CSP14aal • 09:57:39.11 • +12:33:17.70 — Tel. Time: 01h00m

OS 1	WFM-NOAO	Observation
Tel. Time: 900 s Repeat: 4 x Total Tel. Time: 3600s	Instrument Mode: WFM-NOAO-E Telescope Overheads: 360 s	Integration Time: 0 s Instrument Overheads: 0 s Signal/Noise: 0.0

Target • PTF13dwl • 21:16:49.05 • +12:00:50.80 — Tel. Time: 01h00m

OS 1	WFM-NOAO	Observation
Tel. Time: 900 s Repeat: 4 x Total Tel. Time: 3600s	Instrument Mode: WFM-NOAO-E Telescope Overheads: 360 s	Integration Time: 0 s Instrument Overheads: 0 s Signal/Noise: 0.0

Target • SN2013ad • 03:38:41.04 • +10:18:27.22 — Tel. Time: 01h00m

OS 1	WFM-NOAO	Observation
Tel. Time: 900 s Repeat: 4 x Total Tel. Time: 3600s	Instrument Mode: WFM-NOAO-E Telescope Overheads: 360 s	Integration Time: 0 s Instrument Overheads: 0 s Signal/Noise: 0.0

Target • CSP13aaf • 09:55:08.22 • +06:48:31.40 — Tel. Time: 01h00m

OS 1	WFM-NOAO	Observation

Tel. Time: 900 s Repeat: 4 x Total Tel. Time: 3600s	Instrument Mode: WFM-NOAO-E Telescope Overheads: 360 s	Integration Time: 0 s Instrument Overheads: 0 s Signal/Noise: 0.0

Target • CSP13abm • 03:05:59.89 • +04:32:38.20 Tel. Time: 01h00m

OS 1	WFM-NOAO	Observation
Tel. Time: 900 s Repeat: 4 x Total Tel. Time: 3600s	Instrument Mode: WFM-NOAO-E Telescope Overheads: 360 s	Integration Time: 0 s Instrument Overheads: 0 s Signal/Noise: 0.0

Target • SN2013ct • 01:12:54.92 • +00:58:45.70 Tel. Time: 01h00m

OS 1	WFM-NOAO	Observation
Tel. Time: 900 s Repeat: 4 x Total Tel. Time: 3600s	Instrument Mode: WFM-NOAO-E Telescope Overheads: 360 s	Integration Time: 0 s Instrument Overheads: 0 s Signal/Noise: 0.0

Target • CSP13abs • 12:03:06.88 • -01:01:31.70 Tel. Time: 01h00m

OS 1	WFM-NOAO	Observation
Tel. Time: 900 s Repeat: 4 x Total Tel. Time: 3600s	Instrument Mode: WFM-NOAO-E Telescope Overheads: 360 s	Integration Time: 0 s Instrument Overheads: 0 s Signal/Noise: 0.0

Target • LSQ14gfn • 03:28:32.16 • -04:12:14.22 Tel. Time: 01h00m

OS 1	WFM-NOAO	Observation
Tel. Time: 900 s Repeat: 4 x Total Tel. Time: 3600s	Instrument Mode: WFM-NOAO-E Telescope Overheads: 360 s	Integration Time: 0 s Instrument Overheads: 0 s Signal/Noise: 0.0

Target • SN2013gy • 03:42:16.88 • -04:43:18.48 Tel. Time: 01h00m

OS 1	WFM-NOAO	Observation
Tel. Time: 900 s Repeat: 4 x Total Tel. Time: 3600s	Instrument Mode: WFM-NOAO-E Telescope Overheads: 360 s	Integration Time: 0 s Instrument Overheads: 0 s Signal/Noise: 0.0

Target • LSQ11bk • 04:20:44.25 • -08:35:55.75 Tel. Time: 01h00m

OS 1	WFM-NOAO	Observation
Tel. Time: 900 s Repeat: 4 x Total Tel. Time: 3600s	Instrument Mode: WFM-NOAO-E Telescope Overheads: 360 s	Integration Time: 0 s Instrument Overheads: 0 s Signal/Noise: 0.0

Target • LSQ12btn • 09:21:30.47 • -09:41:29.86 Tel. Time: 01h00m

OS 1	WFM-NOAO	Observation
Tel. Time: 900 s Repeat: 4 x Total Tel. Time: 3600s	Instrument Mode: WFM-NOAO-E Telescope Overheads: 360 s	Integration Time: 0 s Instrument Overheads: 0 s Signal/Noise: 0.0

Target • CSP14acl • 01:01:07.04 • -10:18:39.90 Tel. Time: 01h00m

OS 1	WFM-NOAO	Observation
Tel. Time: 900 s Repeat: 4 x Total Tel. Time: 3600s	Instrument Mode: WFM-NOAO-E Telescope Overheads: 360 s	Integration Time: 0 s Instrument Overheads: 0 s Signal/Noise: 0.0

Target • CSP13Z • 10:52:06.06 • -13:34:24.70 Tel. Time: 01h00m

OS 1	WFM-NOAO	Observation
Tel. Time: 900 s Repeat: 4 x Total Tel. Time: 3600s	Instrument Mode: WFM-NOAO-E Telescope Overheads: 360 s	Integration Time: 0 s Instrument Overheads: 0 s Signal/Noise: 0.0

Target • ASASSN-15go • 06:11:30.50 • -16:29:03.52 Tel. Time: 01h00m

OS 1	WFM-NOAO	Observation
Tel. Time: 900 s Repeat: 4 x Total Tel. Time: 3600s	Instrument Mode: WFM-NOAO-E Telescope Overheads: 360 s	Integration Time: 0 s Instrument Overheads: 0 s Signal/Noise: 0.0

Target • LSQ12hjm • 03:10:28.72 • -16:29:37.08 Tel. Time: 01h00m

OS 1	WFM-NOAO	Observation
Tel. Time: 900 s	Instrument Mode: WFM-NOAO-E	Integration Time: 0 s
Repeat: 4 x	Telescope Overheads: 360 s	Instrument Overheads: 0 s
Total Tel. Time: 3600s		Signal/Noise: 0.0

Target • CSP13V • 10:13:10.00 • -16:31:54.00 Tel. Time: 01h00m

OS 1	WFM-NOAO	Observation
Tel. Time: 900 s	Instrument Mode: WFM-NOAO-E	Integration Time: 0 s
Repeat: 4 x	Telescope Overheads: 360 s	Instrument Overheads: 0 s
Total Tel. Time: 3600s		Signal/Noise: 0.0

Target • LSQ12gyc • 02:45:50.07 • -17:55:45.74 Tel. Time: 01h00m

OS 1	WFM-NOAO	Observation
Tel. Time: 900 s	Instrument Mode: WFM-NOAO-E	Integration Time: 0 s
Repeat: 4 x	Telescope Overheads: 360 s	Instrument Overheads: 0 s
Total Tel. Time: 3600s		Signal/Noise: 0.0

Target • ASASSN-14lq • 22:57:19.41 • -20:58:00.8 Tel. Time: 01h00m

OS 1	WFM-NOAO	Observation
Tel. Time: 900 s	Instrument Mode: WFM-NOAO-E	Integration Time: 0 s
Repeat: 4 x	Telescope Overheads: 360 s	Instrument Overheads: 0 s
Total Tel. Time: 3600s		Signal/Noise: 0.0

Target • ASASSN-15da • 05:23:51.880 • -24:42:08.38 Tel. Time: 01h00m

OS 1	WFM-NOAO	Observation
Tel. Time: 900 s	Instrument Mode: WFM-NOAO-E	Integration Time: 0 s
Repeat: 4 x	Telescope Overheads: 360 s	Instrument Overheads: 0 s
Total Tel. Time: 3600s		Signal/Noise: 0.0

Target • SN2014I • 05:42:19.80 • -25:32:39.90 Tel. Time: 01h00m

OS 1	WFM-NOAO	Observation
Tel. Time: 900 s	Instrument Mode: WFM-NOAO-E	Integration Time: 0 s
Repeat: 4 x	Telescope Overheads: 360 s	Instrument Overheads: 0 s
Total Tel. Time: 3600s		Signal/Noise: 0.0

Target • LSQ14ghv • 03:23:44.15 • -31:35:03.17 Tel. Time: 01h00m

OS 1	WFM-NOAO	Observation
Tel. Time: 900 s	Instrument Mode: WFM-NOAO-E	Integration Time: 0 s
Repeat: 4 x	Telescope Overheads: 360 s	Instrument Overheads: 0 s
Total Tel. Time: 3600s		Signal/Noise: 0.0

Target • LSQ14fms • 00:14:59.82 • -51:12:39.54 Tel. Time: 01h00m

OS 1	WFM-NOAO	Observation
Tel. Time: 900 s	Instrument Mode: WFM-NOAO-E	Integration Time: 0 s
Repeat: 4 x	Telescope Overheads: 360 s	Instrument Overheads: 0 s
Total Tel. Time: 3600s		Signal/Noise: 0.0

Target • CSP13aay • 03:25:33.51 • -53:44:19.00 Tel. Time: 01h00m

OS 1	WFM-NOAO	Observation
Tel. Time: 900 s	Instrument Mode: WFM-NOAO-E	Integration Time: 0 s
Repeat: 4 x	Telescope Overheads: 360 s	Instrument Overheads: 0 s
Total Tel. Time: 3600s		Signal/Noise: 0.0

Target • SN2012U • 02:06:04.33 • -55:11:37.50 Tel. Time: 01h00m

OS 1	WFM-NOAO	Observation
Tel. Time: 900 s	Instrument Mode: WFM-NOAO-E	Integration Time: 0 s
Repeat: 4 x	Telescope Overheads: 360 s	Instrument Overheads: 0 s
Total Tel. Time: 3600s		Signal/Noise: 0.0

Target • SN2014eg • 02:45:09.27 • -55:44:16.90 Tel. Time: 01h00m

OS 1	WFM-NOAO	Observation
Tel. Time: 900 s	Instrument Mode: WFM-NOAO-E	Integration Time: 0 s
Repeat: 4 x	Telescope Overheads: 360 s	Instrument Overheads: 0 s
Total Tel. Time: 3600s		Signal/Noise: 0.0

Target • SN2014Z • 01:44:07.99 • -61:07:07.40 Tel. Time: 01h00m

OS 1	WFM-NOAO	Observation
Tel. Time: 900 s	Instrument Mode: WFM-NOAO-E	Integration Time: 0 s
Repeat: 4 x	Telescope Overheads: 360 s	Instrument Overheads: 0 s
Total Tel. Time: 3600s		Signal/Noise: 0.0

Target • CSP14acy • 00:42:28.75 • -64:45:51.00 Tel. Time: 01h00m

OS 1	WFM-NOAO	Observation
Tel. Time: 900 s	Instrument Mode: WFM-NOAO-E	Integration Time: 0 s
Repeat: 4 x	Telescope Overheads: 360 s	Instrument Overheads: 0 s
Total Tel. Time: 3600s		Signal/Noise: 0.0

Target • ASASN-14mw • 01:41:25.16 • -65:37:01.26 Tel. Time: 01h00m

OS 1	WFM-NOAO	Observation
Tel. Time: 900 s	Instrument Mode: WFM-NOAO-E	Integration Time: 0 s
Repeat: 4 x	Telescope Overheads: 360 s	Instrument Overheads: 0 s
Total Tel. Time: 3600s		Signal/Noise: 0.0

Target • CSP13aam • 05:14:47.50 • -66:50:29.10 Tel. Time: 01h00m

OS 1	WFM-NOAO	Observation
Tel. Time: 900 s	Instrument Mode: WFM-NOAO-E	Integration Time: 0 s
Repeat: 4 x	Telescope Overheads: 360 s	Instrument Overheads: 0 s
Total Tel. Time: 3600s		Signal/Noise: 0.0

Target • SN2015F • 07:36:15.76 • -69:30:23.00 Tel. Time: 01h00m

OS 1	WFM-NOAO	Observation
Tel. Time: 900 s	Instrument Mode: WFM-NOAO-E	Integration Time: 0 s
Repeat: 4 x	Telescope Overheads: 360 s	Instrument Overheads: 0 s
Total Tel. Time: 3600s		Signal/Noise: 0.0

Target • CSP15aae • 14:09:55.13 • +17:31:55.60 Tel. Time: 01h00m

OS 1	WFM-NOAO	Observation
Tel. Time: 900 s	Instrument Mode: WFM-NOAO-E	Integration Time: 0 s
Repeat: 4 x	Telescope Overheads: 360 s	Instrument Overheads: 0 s
Total Tel. Time: 3600s		Signal/Noise: 0.0